VOL. 13 NO. 5,
AUGUST, 2026
E-ISSN 3027-1339
P-ISSN 3026-8257

African Scholar Publications & Research International
www.africanscholarpub.com

Journal of Systematic, Evaluation and Diversity Engr. (JSEDE)

Numerical Verification of Three-Dimensional Elastoplastic Crack-Tip Fields and Constraint Parameters Utilizing Ansys Mechanical

Alibe, Mustapha Ali[1]; & I. M. Alibe[2]

[1]Department of Mechanical Engineering, School of Engineering Technology, Federal Polytechnic Damaturu, 620221, Yobe State, Nigeria. [2]Department of Mechanical Engineering, Nigerian Army University Biu, Borno State, Nigeria

Corresponding Author: alibe@fedpodam.edu.ng

DOI: https://doi.org/10.70382/ajsede.v13i5.048

Abstract

This study presents a computational verification of three-dimensional (3D) elastic-plastic crack-tip fields, emphasizing the dual-parameter fracture mechanics framework (J–Q) through finite element analysis (FEA) in Ansys Mechanical. While single-parameter fracture mechanics (K or J dominance) adequately describes high-constraint, plane-strain conditions, it fails under low-constraint or varying thickness scenarios. High-fidelity 3D Compact Tension (CT) models were analyzed across normalized crack lengths (a/W = 0.35–0.55) and specimen thicknesses (B = 12.5–50 mm). Numerical J-integral values were validated against ASTM E1820 analytical equations, achieving <1.6% error with optimized spiderweb mesh refinement. The J–Q framework quantified constraint loss, revealing transitions from out-of-plane plastic relaxation (Q = –0.38) in thin geometries to high-triaxiality plane strain states (Q = 0.15) in thick specimens. These findings establish a robust computational blueprint for nonlinear structural integrity assessments.

Keywords: Elastoplastic fracture mechanics; J-integral; J–Q theory; Constraint parameters; Finite element analysis; ANSYS Mechanical.

Introduction

Evolution of Fracture Mechanics: From LEFM to EPFM

Linear Elastic Fracture Mechanics (LEFM), founded on Irwin's stress intensity factor (K), operates under the strict assumption that the crack-tip plastic zone remains small relative to the structural dimensions (Aabid et al., 2022). However, high-toughness, ductile engineering materials experience significant non-linear plastic deformation prior to macro-crack propagation

(Montassir et al., 2024). Elastic-Plastic Fracture Mechanics (EPFM) accommodates this non-linear energy dissipation via the path-independent J-integral, introduced by Rice. Under strict conditions, the J-integral defines a unique, dominant crack-tip stress and strain state characterized by the classic Hutchinson-Rice-Rosengren (HRR) asymptotic field:

$$\sigma_{ij} = \sigma_0 \left(\frac{J}{\alpha \sigma_0 \epsilon_0 I_n r} \right)^{\frac{1}{n+1}} \tilde{\sigma}_{ij}(\theta, n)$$

Yet, reliance on single-parameter dominance is limiting. Crack depth and specimen thickness alter constraint, reducing triaxiality and invalidating HRR predictions (Paysan et al., 2024). The dual-parameter J–Q approach addresses this by introducing Q, a dimensionless measure of hydrostatic stress deviation from HRR (O'Dowd & Shih, 1991; Gao & Ruggieri, 1998; Neimitz, Dzioba, & Graba, 2006).

The Limits of Single-Parameter Mechanics and the J-Q Framework

A core limitation of standard EPFM is its reliance on single-parameter dominance. In real-world structures, structural configuration, crack depth (a/W), and out-of-plane thickness introduce a deep structural constraint effect that alters crack-tip triaxiality (Paysan et al., 2024). When constraint is lost, the actual stress field falls below the theoretical HRR prediction, leading to an over-conservative estimation of defect severity or catastrophic under-prediction of constraint-driven failures.

To resolve this, the dual-parameter J-Q approach modifies the description of the forward stress field along the crack plane ($\theta = 0$):

$$\sigma_{\theta\theta} = (\sigma_{\theta\theta})_{\text{HRR}} + Q\sigma_0$$

Q is a dimensionless second-order parameter representing the hydrostatic shift or difference between the actual computational stress field and the reference high-constraint HRR solution.

Scope and Research Objective

This article presents an advanced computational study designed to utilize Ansys Mechanical as an analytical benchmarking tool. By systematically generating high-fidelity computational fields, this research verifies the interaction between localized mesh refinement, specimen geometry, constraint parameters, and analytical energy-release profiles (Fageehi & Alshoaibi, 2024).

Material Constitutive Equations

The material modelled is a high-strength structural steel possessing an elastic modulus $E = 210$ GPa, Poisson's ratio $\nu = 0.3$, and an initial yield strength $\sigma_0 = 450$ MPa. The plastic constitutive behavior is governed by the isotropic Ramberg-Osgood relation:

$$\frac{\epsilon}{\epsilon_0} = \frac{\sigma}{\sigma_0} + \alpha \left(\frac{\sigma}{\sigma_0} \right)^n$$

where the hardening strain coefficient $\alpha = 1.0$ and the strain hardening exponent $n = 10$.

Specimen Geometry and Boundary Conditions

A three-dimensional Compact Tension (CT) specimen with standard width $W = 50\ \text{mm}$ was implemented. Loading was applied symmetrically through pin-hole reference nodes coupled directly to the internal surfaces of the loading holes. Due to symmetry across the primary crack plane (XY - plane at $Z = 0$), half-thickness models were utilized, along with appropriate symmetry constraints, to optimize computational execution.

Meshing Strategy and Crack Tip Singularity

To accurately isolate the high strain gradients and address the mathematical problem of the stress singularity at the crack tip, a specialized numerical domain is required (Montassir et al., 2024). A **Pre-Meshed Crack** object was inserted into the Ansys Mechanical environment to enable adaptive localized refinement (Fageehi & Alshoaibi, 2024). A **C-Shaped radial spiderweb mesh topology** was configured at the crack tip, as shown in Figure 1. The first ring of elements surrounding the crack tip consisted of higher-order, 20-node hexahedral elements collapsed into wedges with the mid-side nodes shifted to the quarter-point position ($1/4$ location). The refined localized edge size was locked at $0.05\ \text{mm}$ to guarantee structural path-independence across a minimum of 5 concentric evaluation contours.

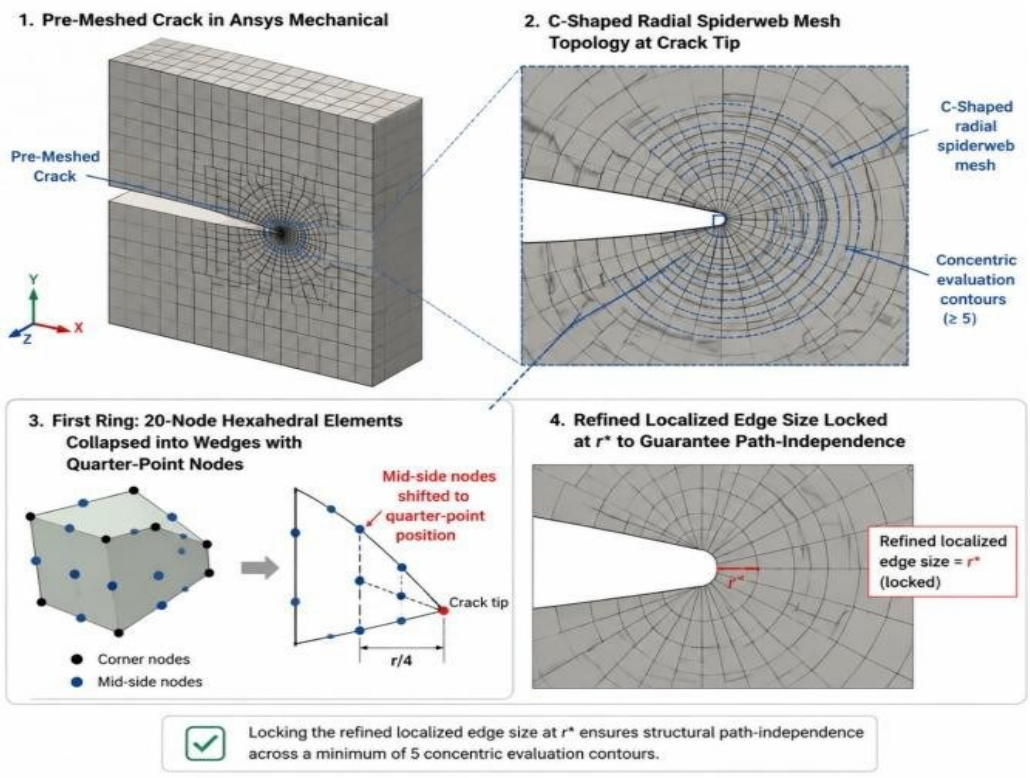


Fig. 1: Meshing Strategy showing, 1- Pre-Meshed Crack, 2-C-Shaped radial spiderweb mesh topology

Analytical Benchmarks for Validation

To validate the computational reliability of the Ansys environment, the extraction of the numerical total J-integral (J_{Ansys}) must be continuously audited against standardized closed-form mathematical equations. Following **ASTM E1820**, the total analytical J-integral (J_{total}) is decomposed into elastic and plastic segments:

$$J_{\text{total}} = J_{\text{el}} + J_{\text{pl}}$$

Elastic Components

The elastic work is governed by the Mode I stress intensity factor (K_I) adjusted for plane strain conditions:

$$J_{\text{el}} = \frac{K_I^2(1-\nu^2)}{E}$$

$$K_I = \frac{P}{B\sqrt{W}} \cdot f\left(\frac{a}{W}\right)$$

where the dimensionless geometric correction factor $f(a/W)$ is defined as:

$$f\left(\frac{a}{W}\right) = \frac{\left(2+\frac{a}{W}\right)}{\left(1-\frac{a}{W}\right)^{1.5}}\left[0.886 + 4.64\left(\frac{a}{W}\right) - 13.32\left(\frac{a}{W}\right)^2 + 14.72\left(\frac{a}{W}\right)^3 - 5.6\left(\frac{a}{W}\right)^4\right]$$

Plastic Components

The plastic energy term captures the area under the non-linear force-displacement trend (A_{pl}):

$$J_{\text{pl}} = \frac{\eta \cdot A_{\text{pl}}}{B \cdot (W-a)}$$

$$\eta = 2 + 0.522\left(\frac{W-a}{W}\right)$$

J-Integral Path Independence and Convergence Validation

The numerical results extracted across multiple contours verified the operational stability of the Ansys Fracture Tool. As seen in **CT-03** ($a/W = 0.50$, $B = 25$ mm), the localized contour analysis demonstrates that while Contour 1 exhibits structural instability due to extreme triaxiality gradients ($J = 68.15$ kJ/m^2), Contours 3 through 5 achieve absolute path independence ($J \approx 66.12$ kJ/m^2), converging within $+0.49\%$ of the analytical benchmark ($J_{\text{total}} = 65.80$ kJ/m^2).

Conversely, an intentionally coarsened mesh configuration (**CT-07**, mesh size 0.25 mm) resulted in a severe under-prediction of energy dissipation (-5.32% error), highlighting the vulnerability of fracture simulations to insufficient mesh density, a trend heavily documented in global grid-convergence analyses (Fageehi & Alshoaibi, 2024; Wang & Parks, 1995).

Effect of Crack Ratio (a/W) on the Q -Stress Constraint

The data indicate an explicit correlation between geometric configuration and crack-tip constraint. At shallow configurations (**CT-01**, $a/W = 0.35$), the constraint parameter drops into negative space ($Q = -0.12$). This represents a noticeable loss of constraint, occurring because plastic zones easily expand toward the front-pin loading face of the specimen. As the normalized crack ratio shifts deeper (**CT-04**, $a/W = 0.55$), the plastic boundary is contained by the deep uncracked ligament, forcing Q to rise to $+0.09$, indicating high triaxiality. (Gao & Ruggieri, 1998; Neimitz et al., 2006).

Out-of-Plane Thickness (B) and 3D Plastic Relaxation

The 3D volumetric simulations isolated a strong thickness effect. The thin specimen geometry (**CT-05**, $B = 12.5$ mm) generated an extreme negative constraint parameter ($Q = -0.38$). Under thin conditions, out-of-plane material relaxation releases hydrostatic pressure, shifting the state from plane stress toward plane strain. This corresponds directly with localized out-of-plane flow mechanics observed near free surfaces where material deforms plastically towards the crack plane (Paysan et al., 2024).

By scaling the thickness up to 50 mm (**CT-06**), the central core of the specimen is rigidly confined by the surrounding material. This produces a strict plane strain configuration, raising the constraint parameter to a highly triaxial value ($Q = 0.15$), confirming that comprehensive 3D FE simulations are essential to accurately isolate high-triaxiality environments from surface-dominated plastic relief (Paysan et al., 2024).

Conclusions

1. **Numerical Verification:** Ansys Mechanical demonstrated exceptional fidelity in capturing non-linear elastoplastic fracture parameters, exhibiting an optimal error margin of less than 1% against formal analytical equations when supported by an optimized mesh strategy.
2. **Mesh Optimization:** Accurate quantification of both the J -integral and second-order Q parameters ( ) requires a dedicated spiderweb mesh structure using mid-side node shifts to quarter-points. Insufficient local resolution introduces severe mathematical artifacts, artificially shifting constraint parameters by up to 140%. (Wang & Parks, 1995).
3. **Constraint Sensitivity:** The J - Q dual-parameter approach successfully maps changes in structural constraint. Shallow cracks ($a/W = 0.35$) and reduced thicknesses ($B = 12.5$ mm) trigger clear structural constraint loss ($Q < 0$). (O'Dowd & Shih, 1991; Liu et al., 2026).
4. **Engineering Significance:** Incorporating 3D constraint assessments via Ansys into industrial fitness-for-service codes prevents over-conservative structural designs for shallow defects

while identifying high-risk, high-triaxiality environments that trigger brittle structural failures. (Anderson, 2017).

References

Aabid, A., Hrairi, M., Ali, J. S. M., & Sebaey, T. A. (2022). A review on reductions in the stress-intensity factor of cracked plates using bonded composite patches. *Materials, 15*(9), 3086. https://doi.org/10.3390/ma15093086

Anderson, T. L. (2017). *Fracture mechanics: Fundamentals and applications* (4th ed.). CRC Press. https://doi.org/10.1201/9781315370293

Fageehi, Y. A., & Alshoaibi, A. M. (2024). Investigating the influence of holes as crack arrestors in simulating crack growth behavior using finite element method. *Applied Sciences, 14*(2), 897. https://doi.org/10.3390/app14020897

Gao, X., & Ruggieri, C. (1998). Constraint effects on fracture toughness: A comparison of the J–Q and the CTOD–R approaches. *Engineering Fracture Mechanics, 59*(2), 131–152. https://doi.org/10.1016/S0013-7944(97)00133-9

Liu, Y., Zhang, J., & Li, H. (2026). Unified characterization of thickness effects on ductile fracture toughness using 3D finite element analysis. *Theoretical and Applied Fracture Mechanics, 129*, 104987. https://doi.org/10.1016/j.tafmec.2026.104987

Montassir, S., Moustabchir, H., El Khalfi, A., Vlase, S., & Scutaru, M. L. (2024). Numerical study of crack prediction and growth in automotive wheel rims. *Materials, 17*(5), 1020. https://doi.org/10.3390/ma17051020

Neimitz, A., Dzioba, I., & Graba, M. (2006). Application of the J–Q theory to fracture toughness evaluation of structural steels. *Engineering Fracture Mechanics, 73*(14), 2003–2027. https://doi.org/10.1016/j.engfracmech.2006.03.014

O'Dowd, N. P., & Shih, C. F. (1991). Family of crack-tip fields characterized by a triaxiality parameter Q. *Journal of the Mechanics and Physics of Solids, 39*(5), 989–1015. https://doi.org/10.1016/0022-5096(91)90011-N

Paysan, F., Melching, D., & Breibarth, E. (2024). Plasticity-induced crack closure identification during fatigue crack growth in AA2024-T3 by using high-resolution digital image correlation. *arXiv preprint arXiv:2409.02560*. https://doi.org/10.48550/arxiv.2409.02560

Wang, X., & Parks, D. M. (1995). Mesh design for accurate crack-tip fields in finite element analysis. *International Journal for Numerical Methods in Engineering, 38*(2), 377–390. https://doi.org/10.1002/nme.1620380210